RESEARCH

Numerical modelling of traffic-induced dynamic loading on a two-story residential building

Henok Marie Shiferaw[1]*, Girma Moges Teshager[1], Solomon Aynalem Hailu[2] and Tadiyos Marie Shiferaw[1]

Abstract

Background This paper presents a numerical modelling procedure of dynamic loading due to traffic on a two-story residential building. In developing countries cities and towns, poor quality narrow road sections with high traffic density are common. In such cases, ground vibration due to traffic could be higher and lightweight buildings located closer are exposed to traffic-induced dynamic loading. Design codes require a proper assessment of such vibrations. However, a clear and definite procedure of assessment is not usually provided. This research presents an assessment procedure of dynamic loading due to traffic on a soil foundation system of light weight buildings based on numerical modeling. Traffic induced ground vibration acceleration amplitudes, frequencies and durations were measured, and the dynamic loads were calculated from measured vibration accelerations and vibrating mass of the vehicle. A two-story residential building with flexible square shallow footings was modelled together with the foundation soil using PLAXIS-2D. The dynamic load was modelled as harmonic loading considering the highest amplitude of vibration measured.

Results On the calculation stage, static loading analysis, dynamic loading analysis and free vibration dynamic analysis were carried out. A maximum increase in extreme total displacement of the soil to 22.03 mm was observed after the dynamic loading from 18.96 mm extreme total displacement due to static loading. Extreme effective mean stress in the soil increased to 112.81 kPa from 110.5 kPa, due to the dynamic loading. In addition, a differential settlement of 3.14 mm between two adjacent footings was observed after the traffic induced ground vibration. Furthermore, the Mohr–Coulomb plastic points were observed to be concentrated to the side of the soil-foundation system which the dynamic load was acting on.

Conclusion The regular exposure to traffic-induced vibrations may cause frequent change in stress and deformation response of the foundation-soil system. In areas where lightweight buildings are exposed to regular traffic induced vibrations, proper assessment of the effect should be carried out and measures should be taken to mitigate the problem. Improving road surfaces and limiting vehicle speed are possible remedial measures to reduce ground vibrations due to traffic.

Keywords Dynamic loading on a building, Traffic-induced ground vibration, Numerical modelling, PLAXIS

*Correspondence:
Henok Marie Shiferaw
henokmarie@yahoo.com
[1] Department of Civil Engineering, University of Gondar, Gondar, Ethiopia
[2] Department of Construction Technology and Management, University of Gondar, Gondar, Ethiopia

1 Background

Vibration is a frequent problem in structures found in urban areas. Common sources of vibration are earthquakes, wind, machinery, elevators, activities of occupants, blasting, traffic and construction operations [1, 2]. The most common sources of artificial ground vibrations in cities and towns are trains, buses, construction

Shiferaw *et al. Beni-Suef Univ J Basic Appl Sci*   (2023) 12:106

Page 2 of 16

activities and machineries. The interaction between vehicles and road surface irregularities creates the vibrations [3]. When the road is rough, the vibration magnitudes due to traffic are detectable [4]. Traffic-induced vibrations are mainly caused by heavy weight vehicles such as buses and trucks. Buildings, bridges, earth-retaining structures and their foundation are exposed to different degrees of vibration caused by traffic. Lightweight vehicles rarely induce vibrations that can be sensed in buildings. The dynamic effect of force generated by the interaction between the wheels and surface irregularities propagates through the soil and can excite foundations and the soil beneath nearby buildings as shown on Fig. 1. When buildings are exposed to such vibrations for prolonged time, the vibration can lead to different degrees of damage on the building. For old and historic buildings, minor damages like plaster cracks can happen more frequently ultimately resulting in major damage [5]. In addition, external shocks induce free vibrations by exciting the natural frequency of the soil-structure system [6]. Vibration measurement and analysis is an important procedure when dealing with vibration problems [5].

In many developing countries, it is quite common to see heavy weight vehicles passing through narrow and damaged road sections where adjacent buildings exist and less care is taken to other activities, which can potentially induce dynamic loading on structures. House owners may face damage on their property due to traffic. People may be concerned and complain about annoyance and building damage. The effect is adverse and long-term on old and historic buildings, particularly those in a weak condition [1, 7].

Narrow and damaged road sections with high volume of traffic, and construction projects through residential areas that use heavy weight vehicles including vibratory rollers and dump trucks, can induce higher ground vibration magnitudes. Such vibrations can be problematic to buildings, wall fences and earth-retaining structures.
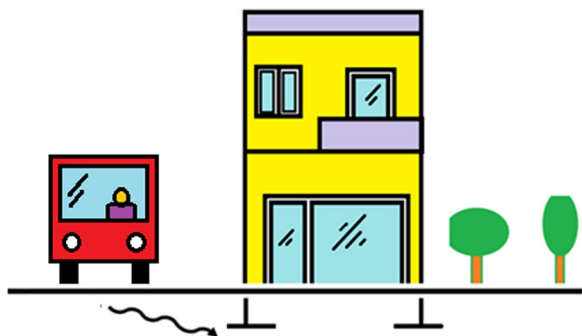
Fig. 1 Schematic representation of traffic-induced vibration acting on the building foundation

The Ethiopian building code of standards for foundations states that, "Foundations for structures subjected to vibration or with vibration load shall be designed to ensure that vibration will not cause excessive settlements." In addition, the code requires assessment of additional and differential settlement caused by self-compaction of the soil [8]. However, there is no clear and definite procedure to assess such vibrations. Thus, the practice is lagging from the code requirement.

There have been some attempts to quantify traffic induced ground vibration and its effect on buildings. Mohannad Mhanna et al. (2012) modelled traffic induced ground vibration numerically and reported that traffic induced ground vibration magnitude is affected by vehicle and road characteristics [9]. Hunt (1991) proposed a stochastic modelling procedure of modelling of traffic induced ground vibration and reported that calculated and measured power spectra for traffic vibrations are comparable [10]. Hong Hao et al. (2001), assessed building vibrations due to traffic and reported that ground vibrations corresponding to normal traffic conditions are not strong enough to cause damage to structures [11]. However, there has been little attempt in modelling the soil-foundation system of light weight buildings. This research addressed the modelling of vibrations caused by road traffic and its effect on a two-story residential building considering the soil-foundation system, through simplified numerical modelling procedure using a commercial software. This research has some potential limitations. It is based on numerical modelling and calculations which might need to be compared with actual data measurements to confirm results. However, numerical modelling procedure is generally acceptable and reliable procedure of modelling soil-foundation systems [12]. In addition, ground vibration magnitudes were measured with a smart phone sensor that has limited capacity; although the accuracy could be acceptable [13].

1.1 Traffic-induced ground vibration

The interaction between vehicles and road surface irregularities creates the vibrations [3]. When the road is rough, the vibration magnitudes due to traffic are detectable [4]. The magnitude of traffic induced ground vibration is small and negligible when compared to other sources of ground vibrations including blasts and earthquakes. Nevertheless, traffic induced ground vibrations should not be neglected completely because the magnitude of traffic induced ground vibration and its effect on structures can be considerable particularly on old and sensitive structures.

Different research indicated that the magnitude of ground vibration depends on the vehicle type, size, speed, road pavement type and condition. Lightweight vehicles

Shiferaw *et al. Beni-Suef Univ J Basic Appl Sci*   (2023) 12:106

Page 3 of 16

on smooth roads induce small magnitudes of vibration amplitudes while heavier vehicles and rough roads create greater vibration. The type of vehicle (weight, suspension system), the type and condition of the road and the speed of the vehicle are some of the parameters that affect the magnitude of vibration amplitudes. Vibration attenuates as it moves away from the source. The distance from the source at which vibration amplitude is being measured is also another parameter that affects the magnitude of vibration amplitude. The factors that influence vibration can be categorized into three. The factors are based on the source, transmission path and receiver as shown in Fig. 2 [3].

Ground vibration measurement is carried out with standard instruments with professionals. Simplified ground vibrations acquisition is also found to be possible using sensors in smart devices (accelerometers in smart devices). With proper applications developed, the sensors in smart devices (e.g., smart phones) can be used to measure some ground vibrations with acceptable accuracy [13].

1.2 Vibration effect on buildings

Ground vibrations cause damages ranging from simple plaster cracks to wall cracks and damages on structural elements of buildings [14, 15]. The damage of vibration on buildings depends on several factors. The two major factors that can be readily identified are the vibration characteristics and the building condition. Vibration is generally characterized by its amplitude, frequency, and duration. The higher the vibration amplitude and duration, the higher the damage it causes on buildings. Filip Pachla et al. [16], studied the effect of vibration duration on reinforced buildings through numerical modelling and reported that short duration vibrations caused small, local cracks while long duration vibrations caused larger cracks and damage on structural elements.

Considering the building condition, sensitive and old buildings are more easily affected by traffic induced ground vibrations, requiring special attention [17]. Haladin et al. [18], studied the influence of traffic induced vibration on earthquake damaged buildings and noted that, although traffic induced vibrations do not damage buildings, such vibrations can contribute to extension of existing cracks. Moreover, the building material and local soil condition plays an important role on building damages where loose site soils are prone to differential settlement [19, 20].

When traffic induced ground vibration is considered, the vibration amplitude and frequency are generally small compared to other sources of vibration. In addition, the duration of vibration is small, lasting in a few seconds also there is a frequent exposure. Nevertheless, light weight, old and sensitive buildings can be easily affected by traffic induced ground vibration of relatively higher magnitudes such as those caused by heavy weight vehicles on rough road surfaces. Moreover, existing damages, such as wall and plaster cracks, can be aggravated because of traffic induced ground vibration.

1.3 Numerical modelling of dynamic loading

Numerical modelling techniques are used to analyse simple and complex boundary and initial value problems in geotechnical engineering that involve small and large deformations. Numerical modelling techniques are useful to analyse the stress and deformation state of a soil-foundation system that happens due to static and dynamic loadings. Several numerical modelling techniques have been developed to approach the problems in geotechnical engineering. The finite element and the finite difference methods are the most widely used methods where the finite element method is usually preferred in calculations for its maturity [12]. Calculations in numerical analysis and in situ measurements of deformations were reported to show good agreement indicating the reliability of numerical modelling techniques [21]. Generally, numerical modelling is considered as a fast, reliable, and powerful tool for a systematic analysis of soil problem.

Several commercial software packages have been developed for modelling and analysis of soils-structures systems one of which is PLAXIS. PLAXIS is a finite element based geotechnical software used to analyse soil deformation problems due to static and dynamic loadings. The simplified, user-friendly input procedures and the improved output facilities provide a detailed presentation of computational results [22].
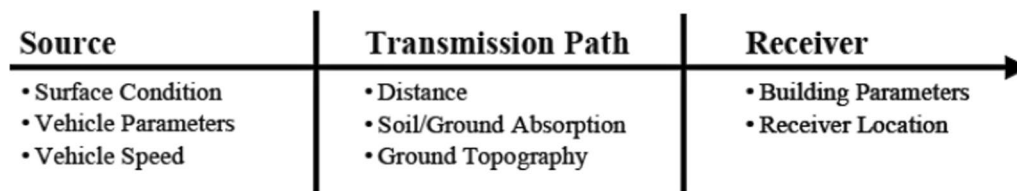
Source	Transmission Path	Receiver
• Surface Condition	• Distance	• Building Parameters
• Vehicle Parameters	• Soil/Ground Absorption	• Receiver Location
• Vehicle Speed	• Ground Topography	

Fig. 2 Main variables influencing traffic induced vibration [6]

Shiferaw *et al. Beni-Suef Univ J Basic Appl Sci*   (2023) 12:106

Page 4 of 16

2 Methods

Ground vibration acceleration amplitudes were measured at different locations using a smart device application called iDynamics. The iDynamics app measures system vibration acceleration amplitude and determines the dominant frequency using the Fast Fourier Transformation (FFT). The iDynamics app is a structural vibration measurement and analysis app developed at a German university, University of Kaiserslautern. The application uses the built-in sensors (accelerometer) of smart devices (smartphones and tablets) to sense vibrations for the purpose of simple vibration measurement and analysis [23].

The accuracy of the data collected using the iDynamics app highly depends on the smartphone it is running. Different smartphones come with different capacity sensors which affect the quality of data. In this study, Samsung

Fig. 3 Schematic representation of traffic-induced ground vibration acquisition
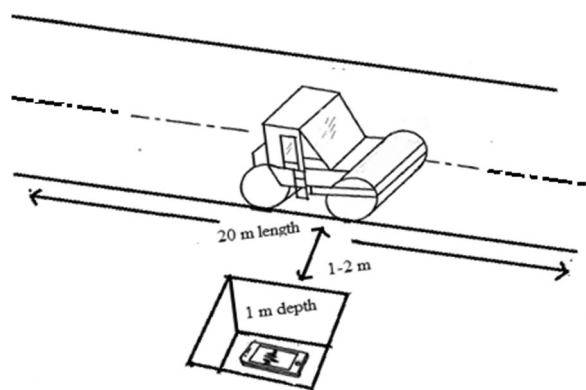
Galaxy J7 Pro smartphone was used. The built-in accelerometer in Samsung Galaxy J7 Pro smartphone has a resolution of 0.0001 g and measurement range of ± 32 m/s^2 which was found to be maximum resolution and range among other smartphones by the time of the research. The resolution and range of measurement of the smartphone was found to be in the range of traffic induced ground vibration [13].

2.1 Ground vibration data measurement

The vibration is measured at 1m depth from the ground to simulate shallow foundation depth. A pit of depth 1 m was excavated adjacent to the roads and the phone was placed parallel to the road where it can measure traffic-induced ground vibration in three axes. The measurement is recorded for about 3 to 6 s i.e., it starts from 20 m from the pit to 20 m away from the pit as shown in Fig. 3.

Vibration amplitude is measured in three axes and the vertical and lateral amplitudes are used in the 2-D numerical modelling. Repeatability of data measured was checked first by taking 10 trail measurements of traffic-induced ground vibration using a single cabin pickup car on asphalt road at 50 km/hr speed. The statistical analysis of data measured gives a coefficient of variation less than 1 as given in Table 1.

Four road surface conditions: asphalt paved, cobblestone paved, gravel and a pothole section of 10 cm depth were considered in ground vibration amplitude measurement. Three types of vehicles, which were, a truck, single cabin pickup and vibratory roller, were used to excite the vibration. The speed of the vehicles was also allowed to vary while vibration was being measured at 1m and 2m distances from the vehicle.

Table 1 Ground vibration acceleration amplitude and dominant frequency

Trial	Acceleration amplitude (m/s^2)			Frequency (Hz)		
	x	y	z	x	y	z
1	0.043	0.029	0.049	3.290	2.810	1.560
2	0.072	0.054	0.117	0.780	3.900	2.340
3	0.065	0.055	0.120	3.687	2.906	2.687
4	0.076	0.055	0.129	1.742	0.781	0.781
5	0.064	0.065	0.173	3.900	2.780	3.780
6	0.068	0.049	0.126	3.170	3.030	0.780
7	0.074	0.048	0.152	2.148	0.781	1.172
8	0.074	0.056	0.115	2.172	1.481	4.297
9	0.059	0.047	0.117	1.758	1.172	1.156
10	0.075	0.055	0.197	2.367	0.977	0.978
Mean	0.067	0.0513	0.1295	1.756	3.517	2.148
Standard deviation	0.010	0.009	0.040	0.987	1.140	1.275
Coefficient of variation	0.151	0.183	0.305	0.562	0.324	0.593

Shiferaw *et al. Beni-Suef Univ J Basic Appl Sci*   (2023) 12:106

Page 5 of 16

The measurement range of Smartphone sensors enabled full acquisition of traffic-induced ground vibration. The amplitudes and frequency contents of traffic-induced ground vibration are in the range of the Smartphone sensor capacity [13]. The major problem in using Smartphone sensors to measure traffic-induced ground vibration was the interference on data measured due to inherent noise vibration of the sensors. For small amplitudes, such as vibration amplitudes induced by lightweight vehicles on smooth roads, the inherent noise vibration can be up to 12% of the external vibration measured. However, for big vibration amplitudes, such as vibration amplitudes induced by a heavy weight vehicle on rough roads, the noise is about 0.09% of the vibration measured [13].

The maximum vibration acceleration amplitudes measured were then used in numerical analysis using PLAXIS. PLAXIS professional version 8 was used to model the soil-foundation system and the dynamic loading due to traffic induced ground vibrations. PLAXIS professional version 8 enables plain strain analysis of dynamic loading. The effect of vibration can be simulated using the dynamic analysis feature of PLAXIS [22]. Only the vibration amplitudes from vibratory roller on a gravel road at working condition (vibration) and truck at a pothole section of a road at 50 km/hr speed were considered in this research. 50 km/hr speed of the truck was selected based on the speed limits of trucks in residential districts and common driving speed of trucks in Ethiopia. in the maximum vibration amplitude and dominant frequency for 2–3 s duration of measurement was used in the analysis.

2.2 Calculation of the dynamic loading due to traffic

The concept of forced vibration was applied to model the ground vibration effect on the building. A spring-mass system can represent a single mode of vibration in a real system. Generally, three types of forcing applied to a spring-mass system can be considered that are;

External Forcing, which models the behaviour of a system that has a time varying force acting on it,

Base Excitation, which models the behaviour of a vibration isolation system where the base of the spring is given a prescribed motion, causing the mass to vibrate and,

Rotor Excitation, which models the effect of a rotating machine, mounted on a flexible floor.

Dynamic loading due to traffic on buildings can be modelled as external forcing. The force is two-dimensional, horizontal (perpendicular to the footing) and vertical. The equation of motion for external forcing of a spring mass system as shown on Fig. 4 is given in Eq. 1.
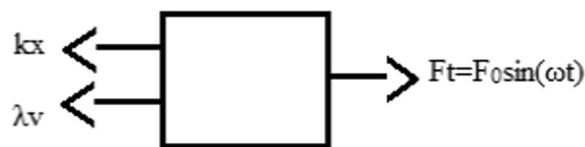

Fig. 4 Dynamic external forcing

$$m\frac{d^2x}{dt^2} = Ft - kx - \lambda\frac{dx}{dt} \tag{1}$$

where m is vibrating mass, x is deformation, Ft is time varying load acting on a system, k is stiffness, λ is viscous damping, $\frac{dx}{dt}$ is velocity of vibration.

Traffic-induced ground vibration amplitude increases as the vehicle approaches the point of interest. Since vehicle speed is considerable, the vibration will be gone shortly after reaching its maximum amplitude. The maximum vibration amplitude is the prime interest since small amplitudes are not significant. Therefore, the maximum vibration amplitude and duration of vibration are considered, and the vibration is simplified to simple harmonic motion, as shown on Fig. 5, to model the dynamic loading.

For a harmonic loading, the time varying force (dynamic load) is given by;

$$Ft = F_0\sin(\omega T) \tag{2}$$

where Ft is the time varying force, F_0 is amplitude, ω is angular frequency given by $2\pi f$, f is frequency in cycles/second, T is duration of vibration.

Substituting Eq. 2 to Eq. 1

$$m\frac{d^2x}{dt^2} = F_0\sin(\omega T) - kx - \lambda\frac{dx}{dt} \tag{3}$$

In PLAXIS harmonic load is defined as;

$$F = MF\sin(\omega T + \varphi 0) \tag{4}$$

where M is Amplitude multiplier, F is Input value of the load, ω is angular frequency, ϕ_0 is initial phase angle in degrees, T is duration of vibration.

In PLAXIS harmonic is applied using harmonic load multiplier. The load magnitude and frequency can be given in terms of "M" and "f" where the active load is given as;

$$\text{Active load} = \text{Dynamic multiplier} * \text{Input value} \tag{5}$$

For input value "F" equal to 1 and initial phase angle "ϕ_0" equal to zero, Eq. 4 can be reduced to;

$$F = M\sin(\omega T) \tag{6}$$

Shiferaw *et al. Beni-Suef Univ J Basic Appl Sci*   (2023) 12:106

Page 6 of 16
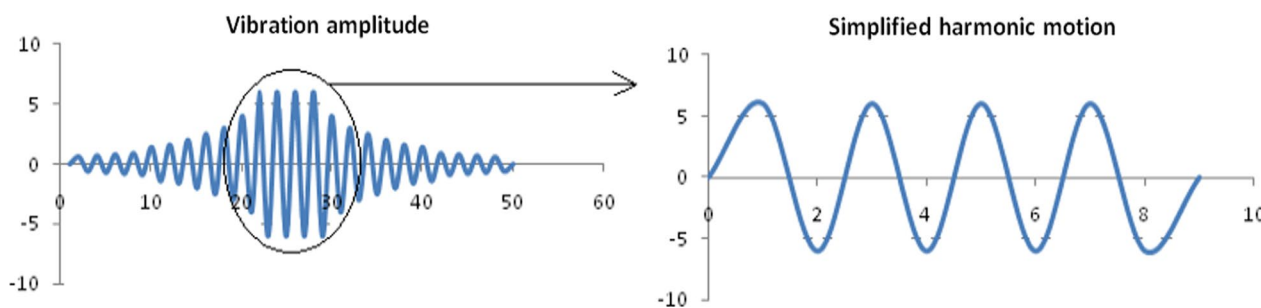
Fig. 5 Schematic representation of vibration simplified to harmonic motion

The left-hand side of Eq. 3 represents dynamic load that can be calculated from measured vibration acceleration and mass, which is equal to the resultant force.

By equating the calculated force to input dynamic load on PLAXIS (Eq. 3 to Eq. 6), the dynamic load amplitude multiplier "M" can be determined from Eq. 7.

$$m\frac{d^2x}{dt^2} = M\sin(\omega T) \tag{7}$$

Thus, calculated forces and dynamic load amplitude multiplier for the two vehicles considered are given in Table 2. The input value, as given in Eq. 4 is equal to 1 which is the resultant of the "x" and "z" direction input values. The "x" and "z" direction input values are calculated as the ratio of the resultant force "F" to the forces in the "x" direction, Fx and in the "y" direction, Fy, respectively. The resultant force multiplied by the input values in both direction gives the forces in each direction respectively.

2.3 Geometric model of footing and foundation soil

The soil-foundation system was modelled in PLAXIS 2D. First the geometric model was created, as shown in Fig. 6, by using the geometric model interface of the PLAXIS 2D and the static and dynamic loads were applied on the model. After creating the geometric model, a necessary boundary condition was set which was a prescribed zero displacements at the boundaries. In addition, a special type of boundary condition, i.e., the absorbent boundary condition, was added for the dynamic loading to avoid wave reflections at the boundaries [22]. Material properties for both the foundation soil and concrete elements

were then added to the model. Mesh was then generated automatically by considering finer mesh sizes around the footing to be able to visualise the deformations of the footings more clearly. A study on deformation of slopes with numerical modelling approach using PLAXIS 2D reported that mesh arrangement induces a 0.5% variation in computed results [24]. In this research mesh independence was addressed by comparing results of two mesh sizes where no considerable difference was observed. Finer mesh sizes gave detailed insights and contours of deformation and stress. The initial stress condition was generated by using K_0 procedure, where K_0 is the ratio of effective horizontal stress to effective vertical stress. K_0 is generally calculated by Jaky's formula (1-sin φ) where φ is angle of internal friction [25]. After generating the initial stress state of the soil, the calculation stage was carried out which includes three calculation phases. The first is plastic calculation due to static loading followed by dynamic analysis due to the considered traffic induced ground vibration which was then followed by calculation of deformation and stress due to free vibration of the soil after the dynamic loading. Results were then viewed for the three phases of calculations i.e., loading conditions, in figures and tables. The soil-foundation system supporting a two-story residential building was simulated in the numerical modelling. The footings considered are flexible footings resting on sand soil deposit.

The software modelling procedure adopted was a recommended procedure by the developers which has been validated and verified with known analytical and semi-analytical solution methods. The primary wave velocity in a one-dimensional confined body which depends on

Table 2 Measured vibration acceleration amplitudes and dynamic load amplitudes

	Mass of vehicle (kg)	ax (m/s²)	az (m/s²)	Fx (kN)	Fz (KN)	F (KN)	f (Hz)	T (s)	M F/(sinωT)	Input values (x, z)
Vibratory roller	12,000	5.001	5.889	60.01	70.67	92.71	12	1	95.77	0.65,0.76
Truck	8,000	0.869	1.126	6.95	9.01	11.38	4	1	26.77	0.61,0.79

Shiferaw *et al. Beni-Suef Univ J Basic Appl Sci*   (2023) 12:106

Page 7 of 16
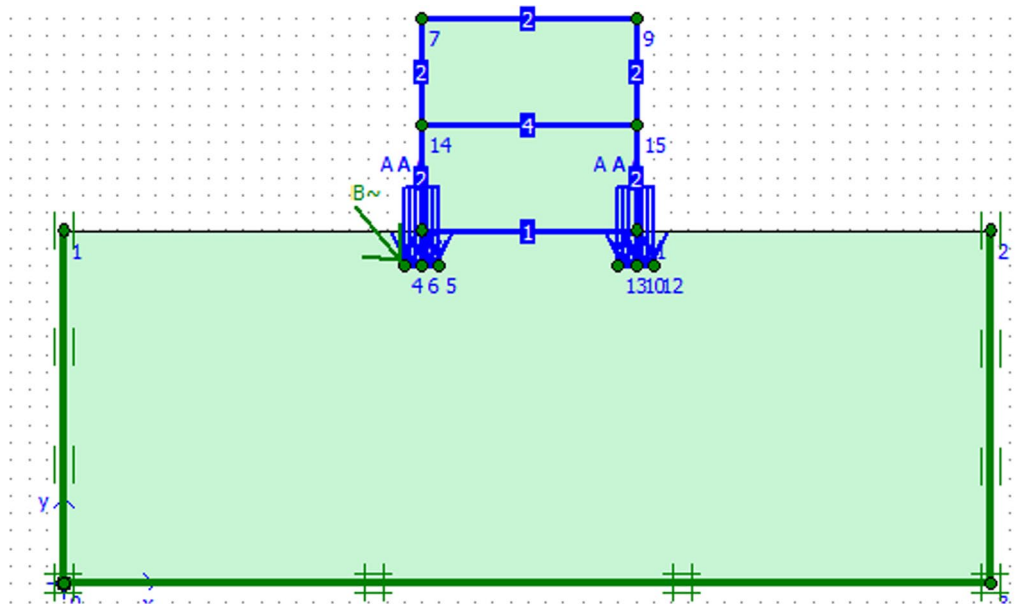
Fig. 6 Soil geometric model for static and dynamic analysis with loading and appropriate boundary condition

constrained modulus, M, and density, of the body is given by Eq. 8.

$$Vp = \sqrt{\frac{M}{\rho}} \tag{8}$$

A 10 m height and 0.2 m radius soil column with given values of constrained modulus and density was modelled with the PLAXIS 2D. The time reach for the wave generated at the top to the middle was determined from both Eq. 8 (Analytical solution) and the numerical modelling. Calculation results for one dimensional wave reach time from the numerical modelling showed good agreement with the theoretical solutions [22].

In addition to one dimensional wave propagation, several numerical solutions of dynamic loads on soils were compared with known analytical solutions that show good agreement with each other.

The load supported by the footings is a uniformly distributed load of 150 kN/m². Presumptive value of bearing capacity for medium dense sand soil was considered while estimating the soil pressure [8]. The model was analysed in three stages. First, the model was analysed under static building load using a plain stress–strain soil model. The stress and deformation due to static column load were determined. At the second stage, the model was analyzed with additional dynamic load due to traffic. In the third stage, dynamic analysis due to free vibration of the soil medium was carried out. Plain strain model with 15 node elements was used in the geometric modelling. The model boundaries should be sufficiently far

from the region of interest to avoid the disturbance due to possible reflection [22]. Thus, 20 m horizontal distance and 10 m vertical distance was considered in the geometric modelling for both static and dynamic analysis. Figure 5 shows the 2-D geometric model of the two-story residential building with static and dynamic loading on PLAXIS. PLAXIS has a standard absorbent boundaries feature which was used to avoid wave reflection from the boundaries.

2.4 Material properties and soil model

The foundation soil is dense gravel soil whose material properties are indicated in Table 3. The building frame and its footings are modelled using plate elements.

The foundation soil was considered to behave elastically, and Mohr–Coulomb (linear elastic model) was used.

Table 3 Material properties and soil model

Soil type	Dense sand
Unit weight	19 kN/m³
C	5 kN/m³
φ	35°
Poisson's ratio	0.3
Elastic modulus	50 MPa
Soil model	Mohr–Coulomb (linear elastic model)
Geometric model	Plain Strain
Rayleigh α and β	0.001, 0.01

Shiferaw *et al. Beni-Suef Univ J Basic Appl Sci*   (2023) 12:106

Page 8 of 16

Dynamic analysis using PLAXIS does not require additional model parameters for dynamic claculations [22]. PLAXIS calculates compression wave and shear wave velocities (Vp & Vs) automatically from soil weight and elastic parameters. Global coarseness mesh was used and the area under the footing is refined two times using line refinement. Ground water table was considered to be well below the footing. Physical damping due to viscous effect is considered using Rayleigh α and β coefficients.

3 Results

3.1 Plastic deformation calculation due to static loading

The first step in the calculation is to determine the total plastic deformation of the soil under static building as shown on Fig. 6. The maximum total deformation was 18.96×10^{-3} m just below the footings (Fig. 7). The maximum vertical displacement under the footings was 18.61×10^{-3} m. The extreme effective mean stress on the soil was 110.5 kN/m^2 at a depth directly below the footings (Fig. 8). Extreme total principal stress was 232.54 kN/m^2. The Mohr–Coulomb plastic points were distributed symmetrically along under both the footings where stress is higher (Fig. 9). In addition, Figs. 8 and 9 show the deformation and stress contours. As shown in Fig. 8, the total deformation is maximum just below the footings and decreases with depth. From Fig. 9, effective mean stress generally increases with depth due to gravity loading and has a higher value under the footings due to superstructure loading. The Mohr–Coulomb plastic points are distributed symmetrically between the two

footings as shown in Fig. 10 which depicts uniform static loading.

The second stage in the calculation is plastic calculation under dynamic loading. Dynamic loads due to the vibratory roller and truck were considered using the dynamic load multipliers calculated.

3.2 Plastic deformation calculation due to dynamic loading

3.2.1 Dynamic loading due to vibratory roller

The deformation in the soil due to the vibratory roller is shown on Fig. 11. As shown on the figure, deformation is different between the two footings. The footing which was directly exposed to the traffic induced dynamic loading experiences greater deformation while the opposite footing experiences less deformation. This could be attributed to damping of the waves in between the distance between the two footings.

The additional maximum total deformation was 22.03×10^{-3} m just below footing 1. The additional maximum vertical displacement was 21.42×10^{-3} m and maximum horizontal displacement was 11.95×10^{-3} m. The maximum extreme effective mean stress under the footings was 112.81 kN/m^2. Extreme total principal stress was 279.29kN/m^2. After the dynamic loading, the plastic points were changed. The plastic points were mainly located around footing one, which is in the near vicinity to the traffic loading as shown on Fig. 12.

The additional vertical deformation under footing 1 was 17.78 mm while under footing 2 was 14.64 mm as shown
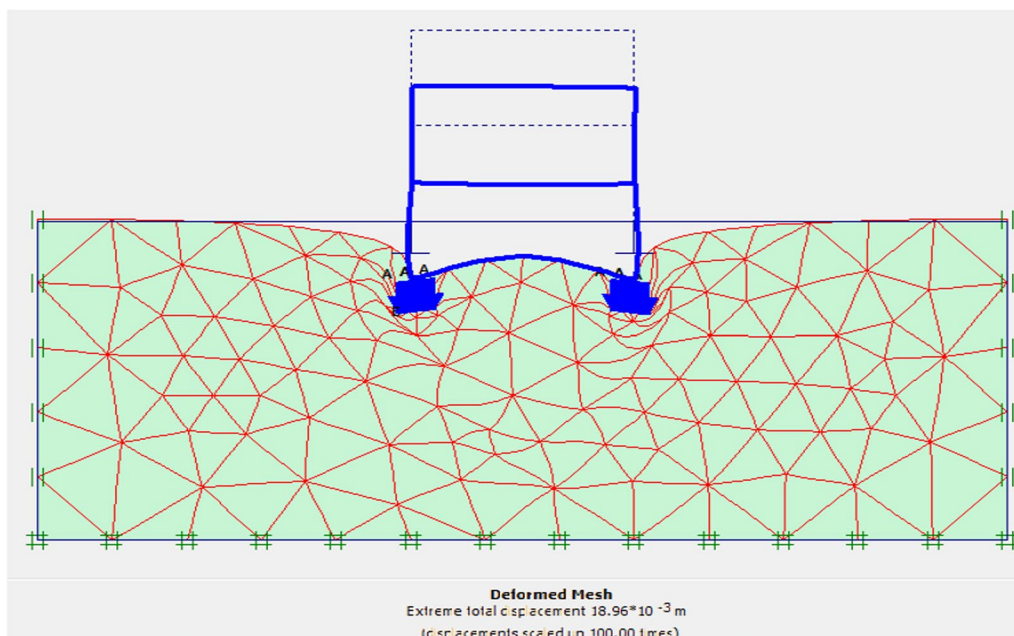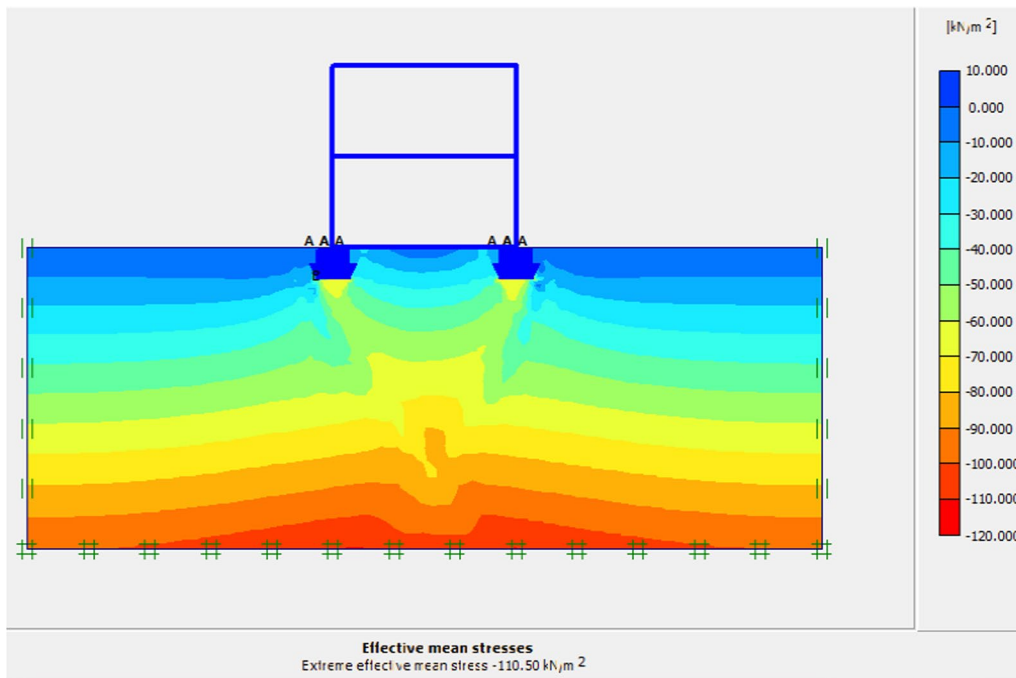

Fig. 7 Deformed mesh under static loading
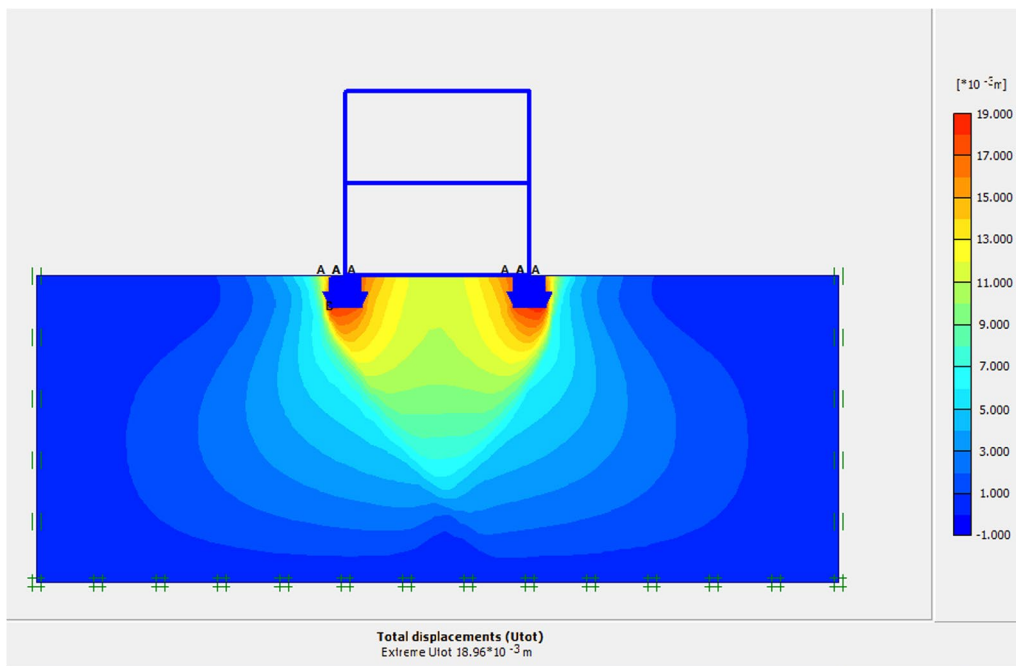
**Fig. 8** Maximum total deformation under static loading

**Fig. 9** Effective mean stress under static loading

on Fig. 13. There is a 3.14 mm difference in settlement between footing 1 and 2 due to the dynamic loading from the roller. This could be due to the rearrangemnt of soil grains under footing 1 due to the dynamic loading which decreases void space thereby causing higher settlement.

The displacement versus time plots on points A, B, C and D which are located at left and right edges of footing
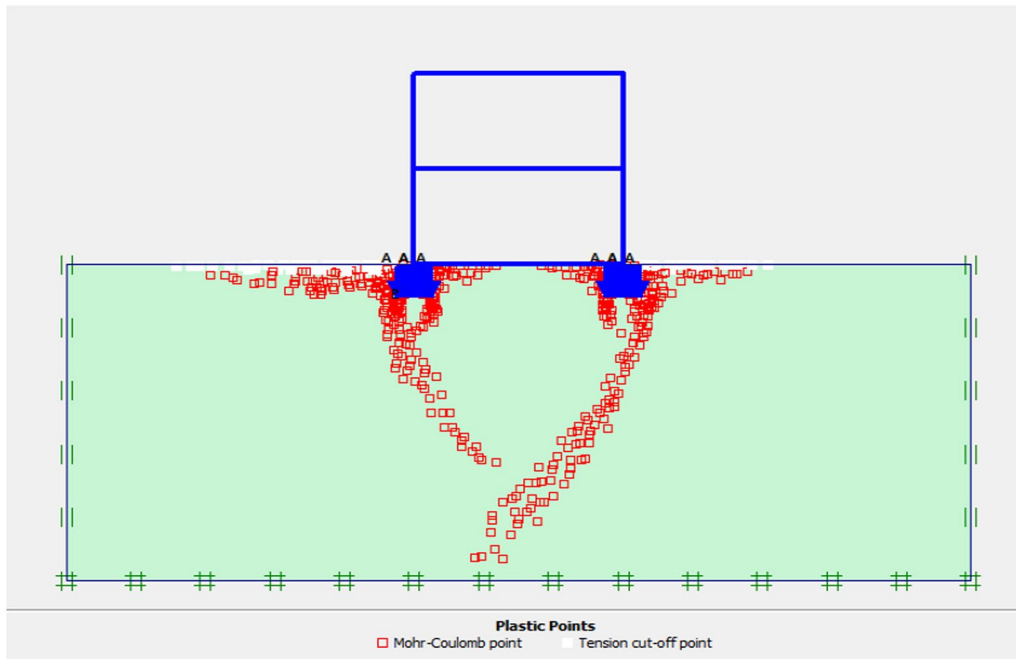
Fig. 10 Mohr–Coulomb plastic points
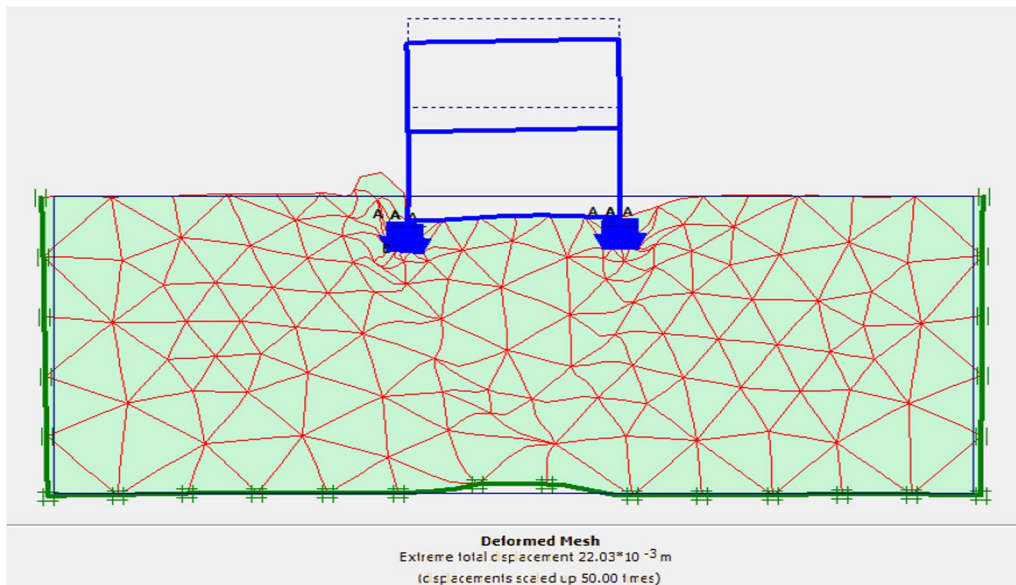
Fig. 11 Deformed mesh under dynamic loading due to vibratory roller

1 and 2 respectively, are shown on Fig. 14. The vibration generally attenuates due to viscous damping after the duration of the dynamic load. It can be seen that there is some permanent deformation due to the dynamic loading as the displacement does not return to zero after the dynamic load duration. The footings were modelled as flexible footings and the calculation indicates that there is a difference in settlement between the different points of the footing, even though the differences are very small (Fig. 14).

3.2.2 Dynamic loading due to truck

The extreme total displacement under the footings due to the truck vibration was calculated as shown on Fig. 15.
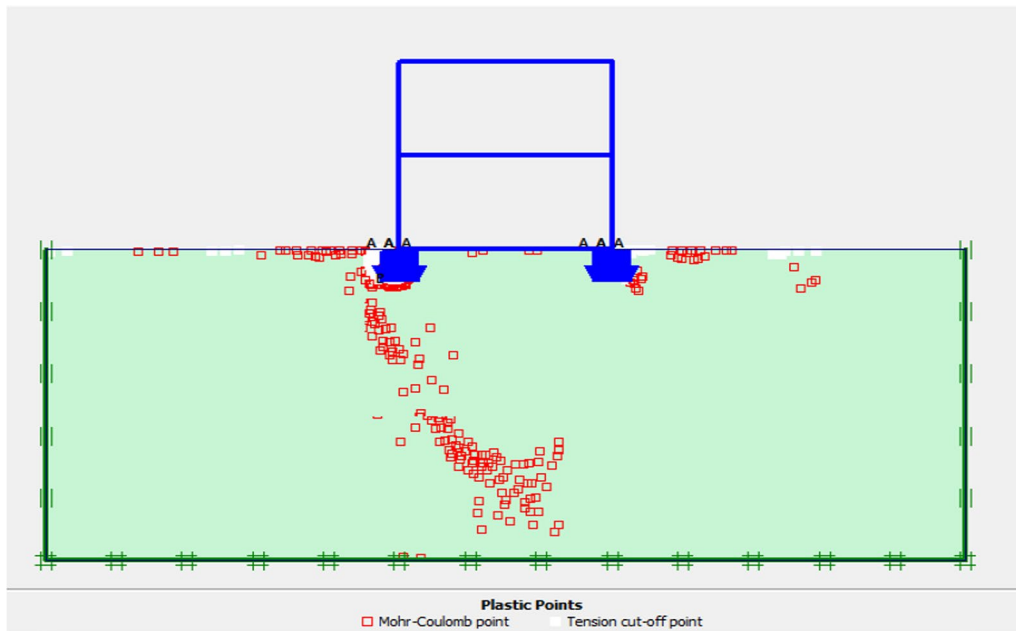
Fig. 12 Mohr–Coulomb plastic points after dynamic loading due to vibratory roller
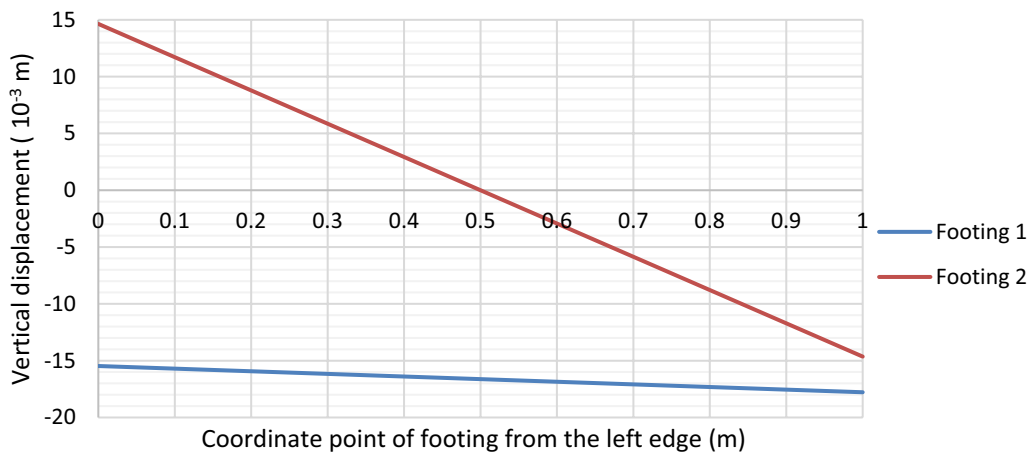
Fig. 13 Vertical displacement under footing 1 and 2

The total displacement under footing one (the footing exposed directly to dynamic loading) is greater. The total additional maximum deformation was 6.88×10^{-3} m (Fig. 15). The additional maximum vertical displacement was 6.39×10^{-3} m downward and maximum horizontal displacement is 4.21×10^{-3} m. As shown in Fig. 16, the total displacement contour is rather non uniform, unlike the static loading, which shows higher values of deformation to the soil foundation system directly exposed to the traffic induced dynamic loading (Fig. 16).

The additional vertical deformation under footing 1 is 6.36 mm while under footing 2 it is 3.9 mm as shown

on Fig. 17. There is 2.46 mm differential settlement between footings 1 and 2 due to the dynamic loading from the truck. The displacement versus time plots for points A, B,C and D are shown on Fig. 18. The displacement attenuates after 1 s which is the loading time of the dynamic load. However there could be some permanent deformation.

3.3 Deformation under free vibration

Free vibration occurs after dynamic load excitation. After the excitation due to the vibratory roller, the vertical deformation under footing 1 increased to 26.85 mm
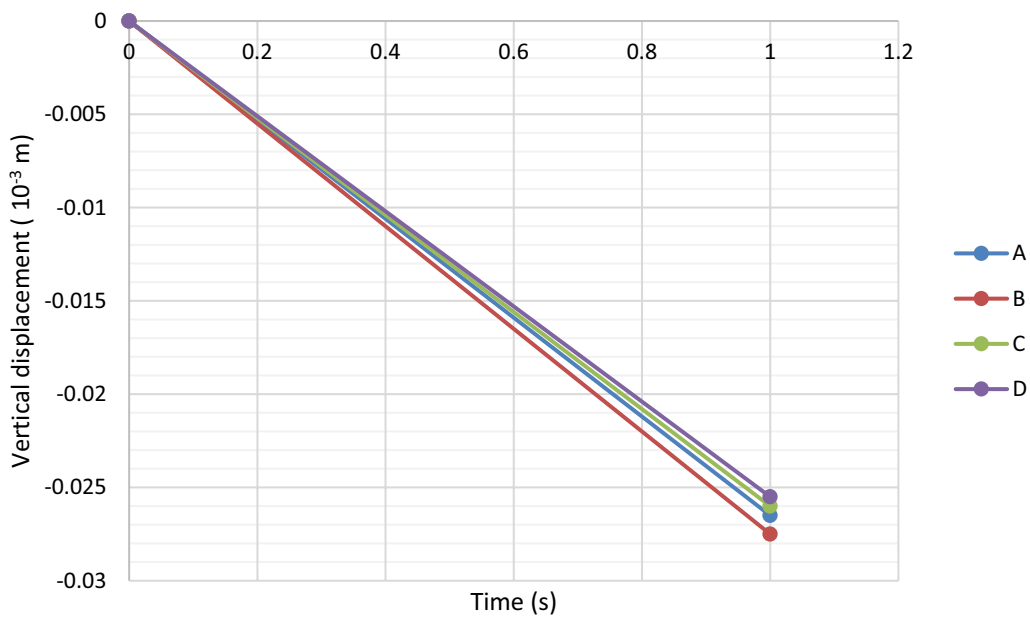
Shiferaw *et al. Beni-Suef Univ J Basic Appl Sci*   (2023) 12:106

Page 12 of 16

Fig. 14 Dynamic displacement attenuation due to material damping

Deformed Mesh
Extreme total displacement 6.88*10 $^{-3}$ m
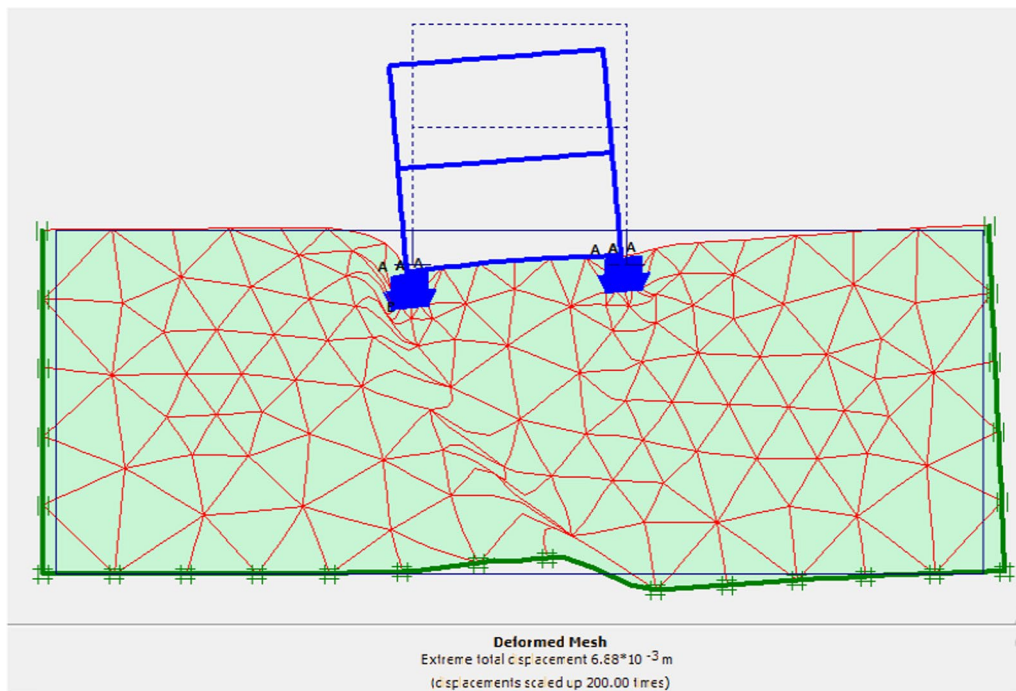(displacements scaled up 200.00 times)

Fig. 15 Maximum total deformation under dynamic loading due to Truck

from 17.78 mm. An increment of 9 mm happened due to the free vibration. The vertical deformation under footing 2 increased to 25.69 mm from 14.64 mm as shown on Fig. 19. The figure shows the total vertical deformation due to dynamic loading and free vibration.

After the free vibration due to the truck, the vertical deformation under footing 1 increased to 11.3 mm from 6.36 mm. An increment of 5 mm happened due to the free vibration. The vertical deformation under footing 2 increased to 6.24 mm from 3.9 mm as shown on Fig. 20.
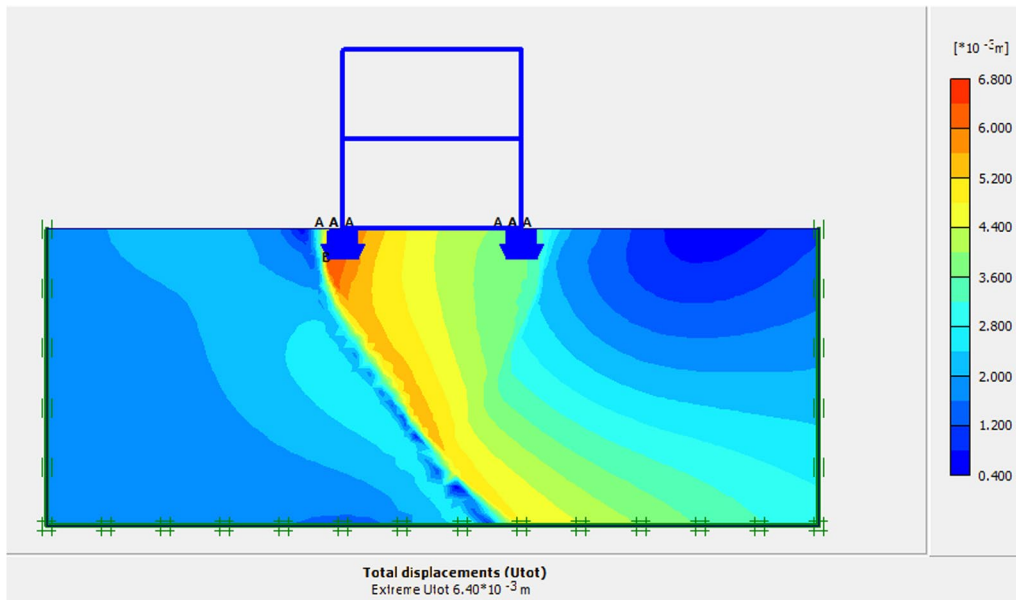
Shiferaw *et al. Beni-Suef Univ J Basic Appl Sci*   (2023) 12:106

Page 13 of 16

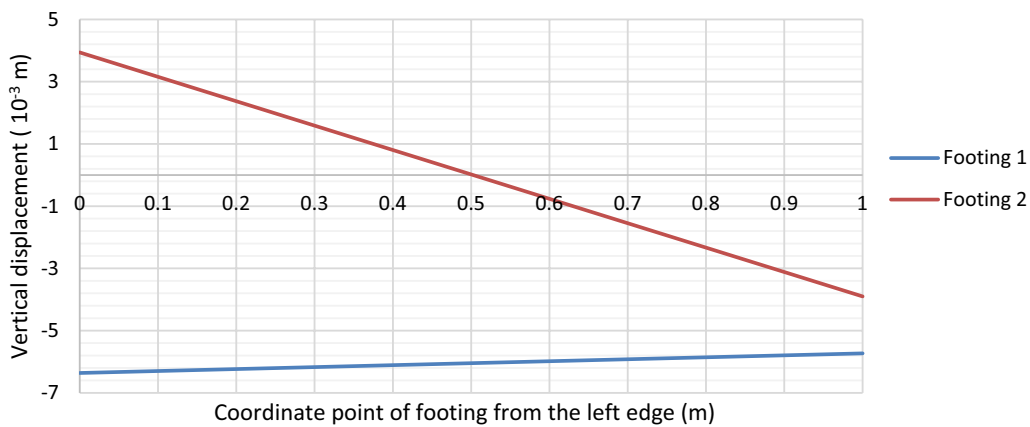**Fig. 16** Total displacement after dynamic loading due to Truck

Fig. 17 Vertical displacement under footing 1 and 2

4 Discussion

Traffic-induced ground vibration amplitude varies with vehicle type, speed, road surface characteristics and distance. The recorded data indicated that vibration amplitude increases with vehicle size, speed and roughness of the road. Vibratory rollers induce higher magnitude of ground vibration.

From the numerical modelling, additional dynamic loading due to traffic caused deformation and stress increase on the soil supporting foundations and structures. Furthermore, the additional dynamic load caused differential settlement between adjacent footings. The PLAXIS analysis result for deformation and stress is summarized in the Table 4 given below.

As given in Table 4, maximum vertical settlement of 17.78 mm was observed under the footings due to the traffic induced ground vibration. The results were comparable to previous studies of settlement due to ground vibration [26–28]. Drabkin et al. [27] studied vibration induced settlement on granular soils and reported that range of observed and calculated settlements caused by soil densification was between 5 and 135 mm.

Numerical techniques can be used to model dynamic loadings due to traffic on buildings. Estimating the dynamic loading accurately and modelling the soil behaviour adequately can improve calculation result quality.

Based on the calculated results, in the case of the vibratory roller, the extreme total displacement induced by the
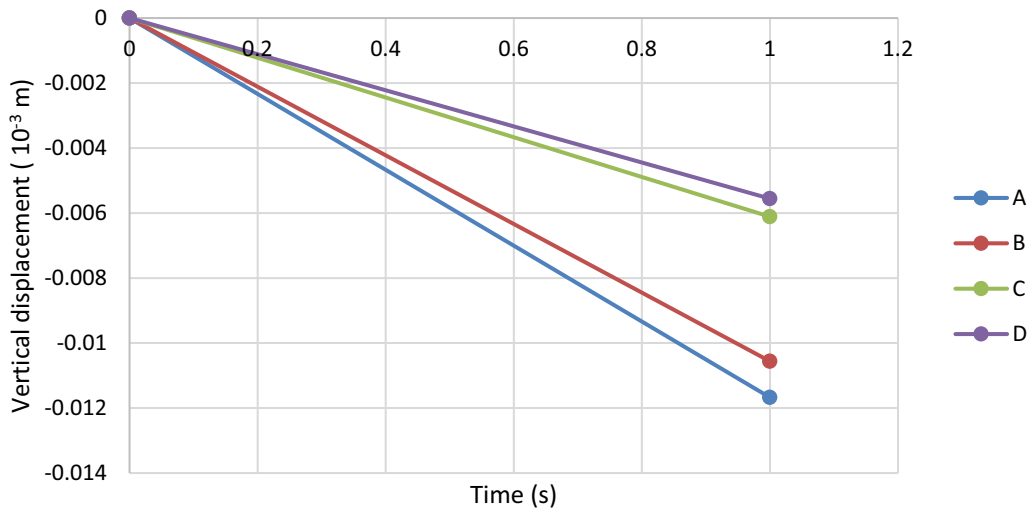
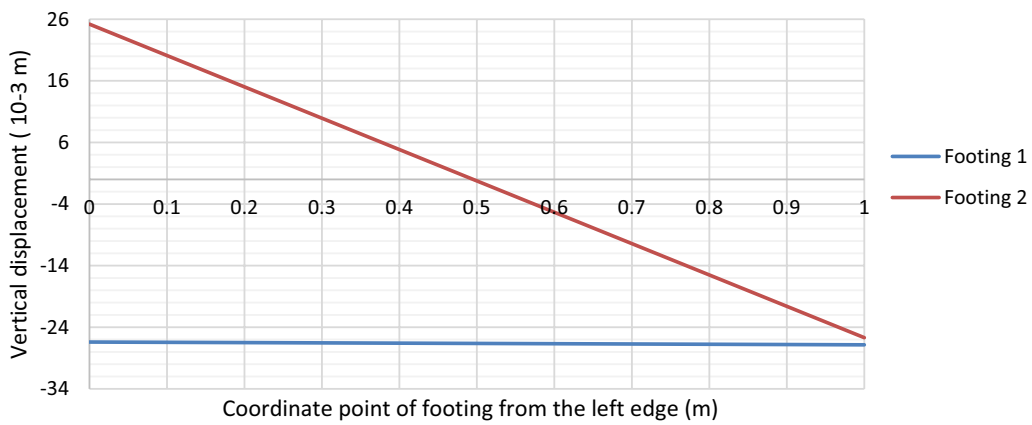**Fig. 18** Dynamic displacement attenuation due to material damping

Fig. 19 Vertical displacement under footing 1 and 2 after free vibration (vibratory roller)
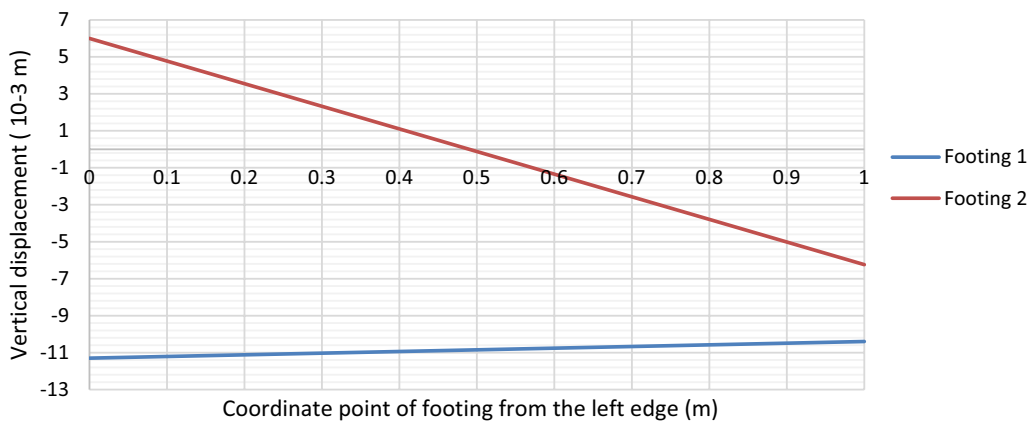
Fig. 20 Vertical displacement under footing 1 and 2 after free vibration (truck)

Table 4 Summary of PLAXIS analysis results

	Static load	Roller		Truck	
		Dynamic load	Free vibration	Dynamic load	Free vibration
Extreme total displacement (mm)	18.96	22.03		6.88	
Extreme effective mean stress (kPa)	110.50	112.81		109.77	
Extreme total principal stress (kPa)	232.54	279.29		228.35	
Maximum vertical deformation under footing 1 (mm)	18.61	17.78	9.03	6.36	4.49
Maximum vertical deformation under footing 2 (mm)	18.61	14.64	11.05	3.90	2.34
Differential settlement between footings 1 and 2 (mm)	0	3.14	-2.02	2.46	2.15

dynamic loading was even greater than the extreme total displacement induced by static loading. 3 mm deformation variation occurs between the two types of loading. The dynamic load due to a vibratory roller can be considerable in many cases and the deformation caused by it can also be significant depending on the type of soil. The dynamic load due to the truck is small compared to the vibratory roller and the deformation due to it is smaller. After the dynamic loading, soil free vibration due to excitation analysis was carried out and the analysis results indicated that the deformation in the soil further changes.

The dynamic load due to the vehicles also changes the stress and plastic points in the soil. Extreme mean effective stress and extreme total principal stress in the soil had increased after the dynamic loading due to the vibratory roller. However, the stresses decreased after dynamic loading due to the truck.

Since the footing near the vehicle was directly exposed to the dynamic loading, it was found to be subjected to higher deformation compared to the opposite footing. Due to this, differential settlement was observed as given in the Table 3 above.

5 Conclusions

Traffic-induced ground vibrations can cause different degrees of fatigue on structures. Heavy weight vehicles through damaged road sections can generate higher magnitude ground vibrations which can reach nearby soil-foundation systems and induce additional dynamic loadings.

Road construction through buildings exposes the buildings to vibrations from the heavy construction vehicles including vibratory rollers. Narrow roads, damaged pavements and roads where vehicle speed and size are not limited can cause relatively higher vibration magnitudes to reach structure foundations.

In this study, traffic induced ground vibration effect on soil-foundation system was studied through numerical modelling technique. Soil-foundation system together with static and dynamic loads was modelled using PLAXIS 2D. Linear elastic constitutive model was adopted in the calculations. The results indicated that traffic induced ground vibrations increased the deformation and stress of the soil-foundation system.

Based on the calculations, an increase in extreme total displacement of the soil to 22.03 mm was observed after the dynamic loading from a value of 18.96 mm extreme total displacement due to static loading. Extreme effective mean stress in the soil increased to 112.81 kPa from 110.5 kPa, due to static loading, after the dynamic loading. In addition, a differential settlement of 3.14 mm between two adjacent footings was observed. The limitation of this research is failure to confirm calculated results with actual filed measurements.

In areas where residential buildings are exposed to regular traffic-induced ground vibration, the magnitude and effect of such vibration should be studied thoroughly and should be kept minimized by improving road surfaces, repairing pothole sections and limiting vehicle speed to elongate useful life of the buildings and their components and avoid unnecessary maintenance costs.

Author contributions
Study conception and design: Henok Marie Shiferaw. Data collection: Henok Marie Shiferaw. Analysis and interpretation of the result: Henok Marie Shiferaw, Girma Moges Teshager, Solomon Aynalem Hailu, Tadiyos Marie Shiferaw. Draft manuscript preparation: Henok Marie Shiferaw, Girma Moges Teshager, Solomon Aynalem Hailu, Tadiyos Marie Shiferaw. All authors reviewed the results and approved the final version of the manuscript.

Shiferaw *et al. Beni-Suef Univ J Basic Appl Sci*   (2023) 12:106

Page 16 of 16

Declarations

Ethics approval and consent to participate
Not applicable.

Consent for publication
Not applicable.

Competing interests
The authors declare that they have no competing interests.

References
1. Hunaidi O (2000) Traffic vibrations in buildings. Construction Technology Update; no. 39. Canada: National Research Council of Canada, Institute for Research in Construction, 2000-06-01. ISSN: 1206-1220
2. Watts GR (1990) Traffic induced vibrations in buildings. In: Transport and road research laboratory, 1990, vol. Research report 246. ISSN: 0266-5247
3. Hajek JJ, Blaney CT, Hein DK. Charlottetown (2006) Mitigation of highway traffic-induced vibration; session on quiet pavements: reducing noise and vibration. In: Annual conference of the transportation association of Canada, 2006. Prince Edward Island, Canada. ISBN: 9781551872250
4. ANSI S3.29 (1983) Guide to the evaluation of human exposure to vibration in buildings. American National Standards Institute, 1983
5. Ertugrul OL, Ulgen D (2010) Attenuation of traffic induced ground borne vibrations due to heavy vehicles. In: International conferences on recent advances in geotechnical earthquake engineering and soil dynamics, 2010. https://scholarsmine.mst.edu/icrageesd/05icrageesd/session02/1.
6. Okumura Y, Kuno K (1991) Statistical analysis of field data of railway noise and vibration collected in an urban area. Appl Acoust 33(4):263–280
7. Jakubczyk-Galczynska A, Jankowski R (2014) Traffic-induced vibrations. In: The 9th international conference "environmental engineering", 22–23 May 2014. http://enviro.vgtu.lt.
8. EBCS (1995) EBCS-7 Ethiopian building code standard for foundations. In: Minstery of works & urban development. Addis Ababa, Ethiopia, 1995
9. Mhanna M, Sadek M, Shahrour I (2012) Numerical modeling of traffic-induced ground vibration. Comput Geotech 39:116–123
10. Hunt HE (1991) Stochastic modelling of traffic-induced ground vibration. J Sound Vib 114(1):53–70
11. Hao H, Ang TC, Shen J (2001) Building vibration to traffic-induced ground motion. Build Environ 36(3):321–336
12. Augarde CE, Lee SJ, Loukidis D (2021) Numerical modelling of large deformation problems in geotechnical engineering: A state-of-the-art review. Soils and Foundations. 61(6):1718–1735
13. Shiferaw HM (2021) Measuring traffic induced ground vibration using smartphone sensors for a first hand structural health monitoring. Sci Afr 11:e00703. https://doi.org/10.1016/j.sciaf.2021.e00703
14. Beben D, Maleska T, Bobra P, Duda J, Anigacz W (2022) Influence of traffic-induced vibrations on humans and residential building—a case study. Int J Environ Res Public Health 19(9):5441
15. Pachla F, Radecki Pawlik B, Stypuła K, Tatara T (2017) Vibration induced by railway traffic-zones of influence on buildings and humans. Vibroeng Procedia 13:188–192
16. Pachla F, Kowalska-Koczwara A, Tatara T, Stypuła K (2019) The influence of vibration duration on the structure of irregular RC buildings. Bull Earthq Eng 17:3119–3138
17. Konon W, Schuring JR (1985) Vibration criteria for historic buildings. J Constr Eng Manag 111(3):208–215
18. Haladin I, Bogut M, Lakušić S (2021) Analysis of tram traffic-induced vibration influence on earthquake damaged buildings. Buildings 11(12):590
19. Papadopoulos M, François S, Degrande G, Lombaert G (2018) The influence of uncertain local subsoil conditions on the response of buildings to ground vibration. J Sound Vib 418:200–220
20. Shijin F, Fuhao L, Xiaolei Z, Guowei D, Jianping L (2021) In-situ experimental investigation of the influence of structure characteristics on subway-induced building vibrations. Earthq Eng Eng Vib 20:673–685
21. Schweiger HF, Fabris C, Ausweger G, Hauser L (2019) Examples of successful numerical modelling of complex geotechnical problems. Innov Infrastruct Solut 4:1–10
22. PLAXIS (2002) Delfit University of Technology & PLAXIS b.v. Plaxis version 8 Dynamic Manual. A.A. Balkema Publishers, 2002
23. Feldbusch A, Sadegh-Azar H, Agne P (2017) Vibration analysis using mobile devices (smartphones or tablets). Procedia Eng 199:2790–2795
24. Shiferaw HM (2021) Study on the influence of slope height and angle on the factor of safety and shape of failure of slopes based on strength reduction method of analysis. Beni-Suef Univ J Basic Appl Sci 10(1):31
25. Delft University of Technology and PLAXIS (2002) PLAXIS Version 8 reference manual
26. Kim DS et al (1994) Prediction of low level vibration induced settlement. ASCE 1–14
27. Drabkin S, Lacy H, Kim DS (1996) Estimating settlement of sand caused by construction vibration. J Geotech Eng 122(11):920–928
28. Kim D-S et al (1996) Prediction technique of vibration induced settlement-on the basis of case studies. Geotechn Eng 12:5

Publisher's Note